β-delayed proton decay of ^{27}P and ^{25}Si: Implications for the ^{26m}Al$(p, \gamma)^{27}$Si reaction rate

I. C. Stefanescu ®,[1] L. Trache ®,[1,*] A. Saastamoinen,[2] B. T. Roeder,[2] A. E. Spiridon ®,[1] A. I. Stefanescu,[1] E. Pollacco ®,[3] G. Lotay,[4] and R. E. Tribble[2]

[1]*Horia Hulubei National Institute for R&D in Physics and Nuclear Engineering, Magurele, 077025 Ilfov, Romania*
[2]*Cyclotron Institute, Texas A&M University, College Station, Texas 77843, USA*
[3]*CEA, IRFU, F-91190 Gif Sur Yvette, France*
[4]*Department of Physics, University of Surrey, Guildford GU2 7XH, United Kingdom*

We report here the results of an experimental study involving the β-delayed proton decay of ^{27}P which was studied with a gas detector, AstroBox2 (AB2), at Cyclotron Institute, Texas A&M University. Five new low-energy proton groups were detected, individual β-proton (βp) branching ratios were calculated for the already known and the new proton groups and an improved half-life of ^{27}P was determined. The discovery of this low-energy protons puts under a new light the reaction rate of ^{26m}Al(p, $\gamma)^{27}$Si. Additionally, a ^{25}Si exotic beam was used for the energy calibration of the detector. In the data analysis of this isotope implantation was ultimately intended to obtain results in accordance with literature in order to validate our method for the analysis of ^{27}P beam, which was finally achieved. Furthermore, an extended description of the analysis method for experiments with AstroBox2 detector is made.

I. INTRODUCTION

In the list of cosmogenic isotopes, ^{26}Al has a special place. Its creation and destruction sites are still under debate, hydrostatic burning stages of low- and intermediate-mass asymptotic giant branch (AGB) stars, classical novae or core-collapse supernovae (CCSN) of massive stars being indicated as possible sources of this element [1]. The temperatures at which these processes occur range between 0.04–0.4 GK in the case of AGB stars, depending on mass, and corresponding to a Gamow energy region of approx. 80–450 keV. Explosive events can also be a source of ^{26}Al; classical novae can reach a peak temperature of 0.3 GK [2], while in the CCSN events the temperatures reach several GK [1]. The discovery of ^{26}Al existence in our galaxy through several studies [3,4] together with a relative short half-life of just 7.17×10^5 yr, which is shorter than the time scale of the galactic chemical evolution ($\approx 10^{10}$ yr) provides evidence that the nucleosynthesis is an on-going process in the Milky Way, and by extension, in the universe.

The level structure of the odd-odd ^{26}Al nucleus is interesting, with a low-spin, long-lived, isomeric state ($T_{1/2} = 6.346$ s and $J^\pi = 0^+$) at just 228.3 keV above its ground state ($J^\pi = 5^+$) [5]. They are members of the same $\pi d5/2 \times \nu d5/2$ multiplet. The β^+ decay of the ground state populates an excited state in ^{26}Mg which then decays by emitting a γ ray with an energy of 1.809 MeV, while the isomer β^+ decays with overwhelming probability to the ground state of ^{26}Mg [5], one of the almost pure superallowed Fermi transitions known and well studied.

The presence of this isomer complicates the total economy of any nucleosynthesis calculations involving the production and destruction of ^{26}Al in stellar processes. Due to the significant difference in angular momentum between the two states (i.e., very small γ-ray decay constant with a mean lifetime of $\approx 10^5$ yr) the direct γ-ray transition between the isomer and ground state is strongly inhibited. In nucleosynthesis calculations at temperatures lower than $T = 0.4$ GK the two states are treated as two different species.

The destruction of both states is accomplished mainly through radiative proton capture (p, γ) to excited states in ^{27}Si over the proton emission threshold $[S_p = 7.46334(13)$ MeV corresponding to ^{26g}Al and, respectively, $S_{p'} = 7.69164(13)$ MeV for ^{26m}Al] [6] and is dominated by resonances. Therefore, the spectroscopy of these resonances is sufficient to evaluate the reactions rates. Their properties—energy, spin-parity, and resonance strength—are of particular importance since the reaction rates of ^{26g,m}Al$(p, \gamma)^{27}$Si depend critically on them.

These processes have been investigated extensively in the last decades through theoretical studies [7] and various experiments which highlighted the proton capture either on the fundamental state [8–11], on the isomer [12–15], or on both [16].

When the capture is dominated by resonances, the reaction rate at temperature T is the incoherent sum of the contributions of each narrow resonance, as it will be detailed in Sec. IV D. Therefore, the evaluation of the contribution to the reaction rate can be done from the spectroscopy of these resonances.

One investigation method that can offer an insight on the excited states of ^{27}Si corresponding to a resonance in the proton capture on ^{26m}Al is the β-delayed proton decay of ^{27}P.
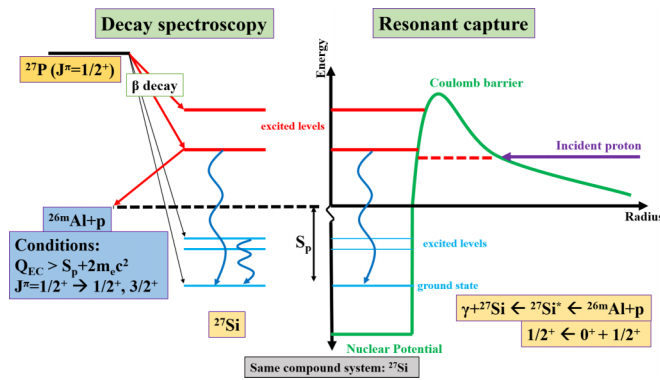
---

*Contact author: livius.trache@nipne.ro

FIG. 1. Schematic draw of the indirect method used to study the resonances in the ^{26m}Al(p, γ) ^{27}Si. The incident proton will be captured on ^{26m}Al and will populate excited states in ^{27}Si. However, the same states can be populated through the β decay of ^{27}P. If these levels are above the proton separation threshold, S_p, then they have a probability to decay by proton emission competing with γ-ray emission (curved arrows), if the selection rules are met and if there is enough available energy for the β decay.

The ground state of ^{27}P ($J^\pi = 1/2^+$) will β^+ decay and populate preferentially low spin states in ^{27}Si ($J^\pi = 1/2^+, 3/2^+$). If the excited levels lie above S_p, then there is a chance of a proton being emitted. The energies of these protons in the center of mass (c.m.) system represent the actual resonance energies of the system ^{26m}Al(p, γ) ^{27}Si and the low-energy ones (below 450–500 keV) are of interest in the astrophysical temperature range, and are sought in this work. This indirect method is well described in [13,17]. A schematic draw of this process is presented in Fig. 1. Three previous studies have shown that ^{27}P is a β-delayed proton emitter: Aystö *et al.* [18], Ognibene *et al.* [19], and McCleskey *et al.* [13]. However, none of them was able to detect protons below $\approx$450 keV, energy range for resonances important in nuclear astrophysics, because of the high accompanying positron background and small βp branching ratios (β decay followed by proton emission).

We report here an experiment in which we managed to overcome the difficulties posed by the presence of the large positron background in our detection system and we successfully investigated the β-delayed proton decay of ^{27}P. We located five new low-energy proton transitions, measured their branching rations, evaluated the proton partial widths of these resonances and the corresponding reaction rate of ^{26m}Al(p, γ) ^{27}Si at temperatures up to 1.0 GK is proposed.

II. EXPERIMENTAL TECHNIQUES AND SETUP

The experiment we report here was part of a program developed after 2006 at the Cyclotron Institute, Texas A&M University with the objective of measuring properties of nuclei that exhibit beta-delayed proton decay important for nuclear astrophysics and nuclear structure studies. Emphasis was placed on measuring very low energy protons, $E_p = 100$–500 keV. Two basic problems occur when attempting that: low energy protons are not easy to detect due to an overwhelming background from positrons and the very low probability of proton decay at low energies due to a decreasing barrier penetrability with the decrease of their energy. Three basic improvements have been made in these studies: (i) a very good separation of the radioactive β-delayed proton emitting nuclei using the MARS spectrometer [20]. Secondary beams of 30–40 MeV/nucleon were obtained; (ii) the emitter was implanted directly in the proton detector to avoid energy losses of emitted protons in various dead layers—initially in very thin silicon-strip detectors. The implantation was realized and the depth of it was controlled with a simple rotating energy degrader in front of the detector; (iii) later, gas was used as detector in order to diminish the signal from the overwhelming number of positrons emitted. A MicroMEGAS (MM) [21] was used as a special signal amplifier. This allowed us to reach the goal of measuring proton with energy as low as ≈ 100 keV and β-proton (βp) branching ratios down to 10^{-6}.

The emitters under study are short lived, of the order of hundreds of milliseconds. The basic technique consists of using implantation/measurement cycles (beam-on/beam-off), i.e., the primary beam from the K-500 superconducting cyclotron is pulsed in macropulses. In the first part, the secondary beam that contains the nucleus of interest is produced, selected, then implanted and stored in the very active volume of the detector (beam-on). Later the decay of that specific nucleus is measured (beam-off). The duration of each step was chosen to be twice as long as the half-life of the nucleus of interest (hundreds of ms). Very good results were obtained for various nuclei such as ^{23}Al, ^{31}Cl, ^{20}Mg, ^{35}K, and ^{27}P [13,17,22–24].

The secondary beam for the experiment reported in this paper was produced in-flight through a ($p, 2n$) reaction in inverse kinematic by bombarding a liquid-nitrogen-cooled hydrogen target with a primary beam of ^{28}Si at 40 MeV/nucleon. The target was kept at a pressure of 2 atm in a 90 mm long stainless steel cylinder with 4 μm-thick Havar in- and out-windows. The reaction products were transported and separated with MARS resulting in a beam of ^{27}P with $\approx$55% purity at 36 MeV/nucleon and a momentum spread of $\delta p/p = \pm 0.25\%$ at the end of MARS where a ΔE-E silicon telescope (1 mm and 500 μm thickness, respectively, and colloquially named *target detector*) was placed in the focal plane to check the secondary beam composition and select ^{27}P. At this point the beam intensity was reduced to protect the target detector. The particle identification (PID) in this telescope is shown in Fig. 2 and two situations are presented when: (i) the last pair of vertical and horizontal slits is fully open and (ii) vertical slits of the last pair are partially closed at a position to allow only the central part of the beam containing ^{27}P to go through. After the PID is established and the slits are locked into the final position, the target detector is removed from the beam path, the primary beam intensity is increased and the PID is checked again inside the implantation detector.

For this experiment we used a gas detector, AstroBox2 (AB2), largely described in [25], which is an upgraded version of AstroBox1 [26]. No specific details other than the ones of interest for the present experiment will be given here. The detector was filled with ultrahigh purity P5 gas (Ar:CH4 95%:5%, grade 5.0, Praxair) which was kept at a pressure
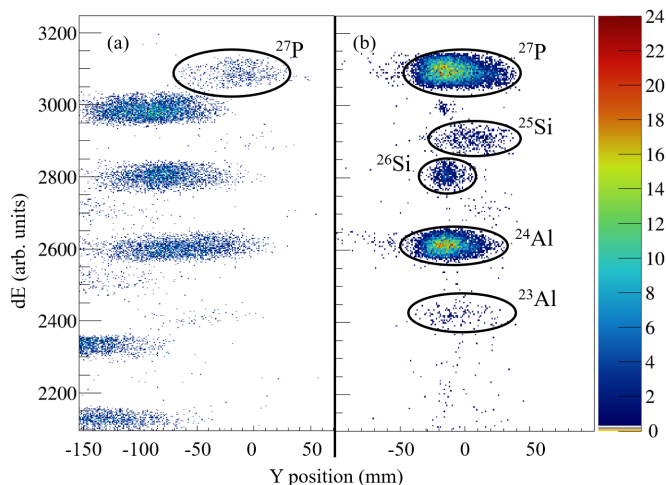
FIG. 2. (a) PID in target detector when the last pair of vertical and horizontal slits are fully open; (b) PID when the vertical slits are closed to $+3.16$ mm/ -2.27 mm. The composition of the secondary beam was: ^{27}P 55%, ^{24}Al 35%, and 10% the other nuclei indicated in (b).
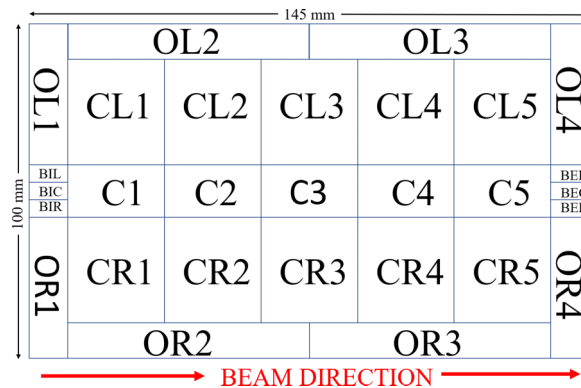

FIG. 3. Schematic drawing of the MM amplifier pads. Total number of pads is 29, the most important in data analysis being the central ones, labeled: C—central, CL—central left, and CR—central right. The central left/right are the most powerful pads to clean in data analysis the very central region of any positron background.

of 800 torr during the experiment. To implant the nuclei of interest into the detector, the beam was passed through a rotatable Al degrader with a thickness of 546 μm and an aramica window of the gas detector of 76 μm thickness.

After the beam of the radioactive species of interest is stopped in the gas volume of the detector, we cut the implantation and wait for their decay. The electrons produced by the decay radiation through ionization are drifted in an electric field created between a cathode and the grounded micromesh towards the MicroMEGAS amplifier, which itself is the anode. The detector itself is an ionization chamber and only the MicroMEGAS qualities give a stronger signal and a good resolution. The amplifier we used is divided into 29 regions (pads), the most important being the inner 15 central pads, with 145 mm×105 mm total dimension. A schematic drawing of the MicroMEGAS amplifier's anode used in this experiment, in which the pad layout is presented, can be seen in Fig. 3.

The resulting implantation rate was about 800 pps for ^{27}P. The main contaminant was ^{24}Al ($\approx 35\%$); other species as ^{28}P, ^{25}Si, ^{26}Si, and ^{23}Al could be found in the final beam, but none of them represented an issue in the overall measurements, as it will be explained below.

The implantation is controlled to stop ^{27}P over the desired pads, usually the most central ones (C3 and C4, see Fig. 3), with the help of the rotatable Al degrader and the small initial momentum distribution. The degrader angle in this experiment for ^{27}P was 28°. Since all the nuclei in the cocktail beam have the same magnetic rigidity and velocity at entrance, the lower Z contaminants pass through the gas and stop well beyond the region of interest, as it is the case of ^{23}Al, whereas higher Z impurities are stopped before they reach the active volume. The PID in AB2 can be seen in Fig. 4. A small trace of ^{24}Al can be observed stopping in the gas region corresponding to the C5 pad. However, for the sensitive case where the branching ratios were determined, this pad was

excluded from the data analysis to avoid any ^{24}Al interference since it is a β-delayed charged particle emitter.

Electronic signals (beam-on and beam-off requests, corresponding to the implantation/measurement cycle) were sent to the cyclotron in order to get a pulsed beam. ^{27}P was implanted for 600 ms into the gas volume, with a 5 ms wait to allow the cyclotron to receive the beam-off request and to change the conditions of our electronics; the decay was measured also for 600 ms, roughly twice the known half-life value 260(80) ms [18]. The energy loss of the ions in the implantation mode and of the emitted protons in the measurement mode are very different, therefore we had to adjust the electronics for these two different dynamic ranges of signals: 0–100 MeV and 0–1000 keV, respectively. In order to limit the transmission of the drifting electrons towards the MicroMEGAS anode during implantation phase, a PCB with 50 μm thick wires, forming
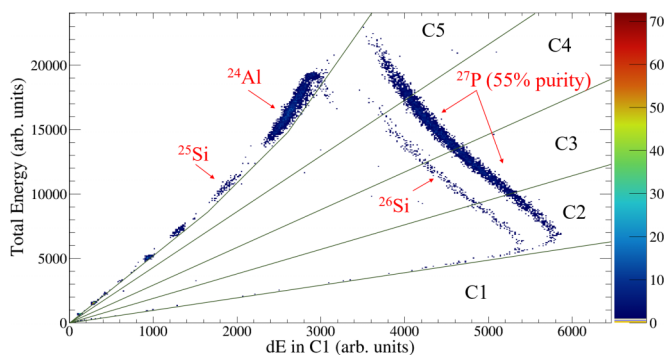

FIG. 4. The total energy deposition of the central pads (C1–C5) versus the energy loss in the first pad (C1) during implantation phase. The picture is obtained with the Al degrader positioned at an angle of 28° and was the final setting used for the experiment. Implantation is centered over C3,C4 pads, with some tails over C2 and C5. ^{26}Si is also stopped in the same area as ^{27}P, but it is not a β-delayed proton emitter so this was not an issue in the decay measurement. All the other contaminants are punching through and not stopping in the interest area of the detector.
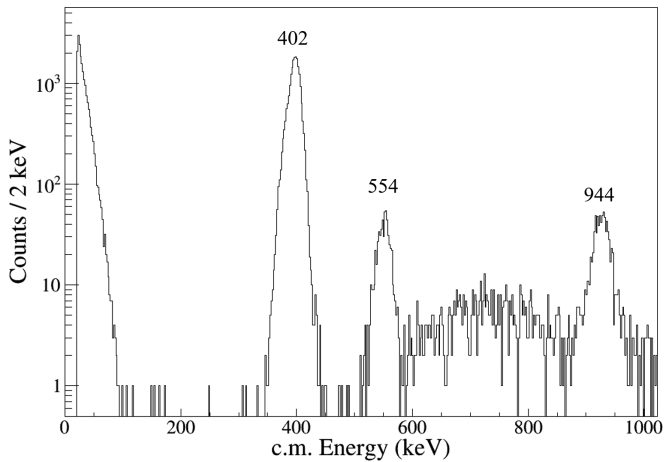
FIG. 5. Measured β-delayed proton spectrum of ^{25}Si in the most central pad, C3 (M = 1 condition applied). The positron background reduction down to $\approx$80–90 keV is clearly visible.

FIG. 6. Decay time spectrum of ^{25}Si, obtained during beam-off; it was gated by the decay energies of 402, 554 and 944 keV proton peaks.

a gating grid, was placed just above the anode. The voltage of the gating grid was pulsed between +46 V (beam-on) and −330 V (beam-off) and synchronized to the cyclotron beam pulsing.

The gating grid setting of +46 V was chosen experimentally for partial transparency to allow counting of the implanted ions during the beam off period without intervening on the MM voltages.

III. DATA ANALYSIS

A. Energy calibration

The energy calibration was done with well known β-delayed protons from the decay of ^{25}Si, with energies of 402(1) keV, 554(5) keV, and 944(1) keV [27]. The secondary ^{25}Si beam was obtained in the same experiment through the fragmentation of the primary beam of ^{28}Si at 40 MeV/nucleon, in the same way as for obtaining ^{27}P, but bombarding a solid 279 μm thick Al target. After the secondary beam composition was confirmed with the ΔE-E silicon telescope at the focal plane of MARS, the obtained ^{25}Si beam was deliberately defocused and the momentum spread of the secondary beam increased to $\delta p/p \approx 1.75\%$ to allow a broad and relatively uniform distribution for ^{25}Si over all 15 inner pads of AB2. An intensity of almost 25 pps was obtained; even though it seems relatively low, the fact that ^{25}Si has a high β-proton branching ratio (almost 35%) allowed us to achieve enough statistics in just 8 hours of continuous run.

The proton spectrum acquired can be seen in Fig. 5 and it was obtained with an analysis procedure by using a multiplicity = 1 condition (M = 1), which will be detailed in Sec. III B. Similar spectra are acquired for all the larger pads in the central area and even for most of the outer pads. This gives energy calibrations for all elements. Along with the well known proton groups, we observe a low intensity group between 554–944 keV. Even though a recent study of Sun *et al.* identified the peak as a new proton group with the energy of 724 keV [27], its origin is not so well understood in our
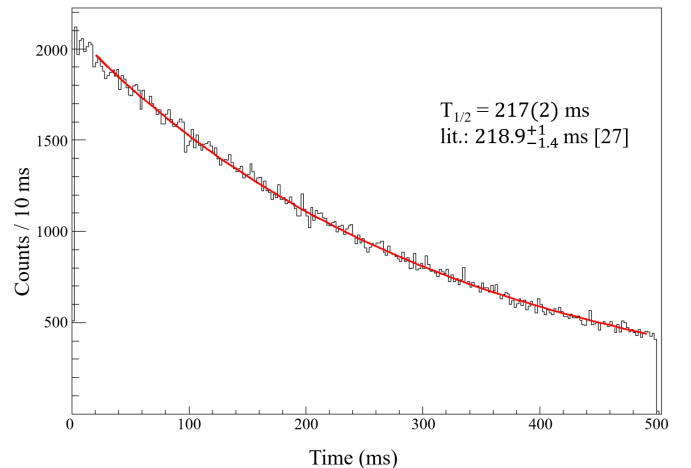
study. It looks more like a group of several peaks at similar energies, not easy to resolve. Since we used the ^{25}Si beam mainly for energy calibration of AB2, the presence of this low intensity group was not further investigated. Furthermore, the 554(5) keV energy peak position was determined with better precision than previous study of Sun *et al.* [27].

The half-life of ^{25}Si could also be determined. By using a 10 kHz clock to timestamp the events, a decay time spectrum was constructed by gating on the proton energies of interest. By exponentially fitting this data (see Fig. 6), a 217(2) ms half-life was obtained, a result which is in good agreement with the latest study [27]. βp branching ratios were obtained for the detected proton groups and are listed in Table I. We conclude that the differences in branching ratio values arise from our reduced positron background compared with other studies [27,28]. Note the lack of background in spectrum between 100–400 keV.

B. Constructing the multiplicity conditions

The geometrical construction of the MicroMEGAS amplifier provides an important advantage in what concerns the data analysis. Specifically, different multiplicity conditions can be applied between the pads that are hit (colloquially, any signal firing a pad is called a hit). The β-delayed proton spectrum

TABLE I. ^{25}Si β-delayed proton energies, in c.m., and their associated βp branching ratios, which are compared with previous studies. Branching ratios are determined by summing up multiplicity M = 1, 2, and 3 data. Energy values as in [27].

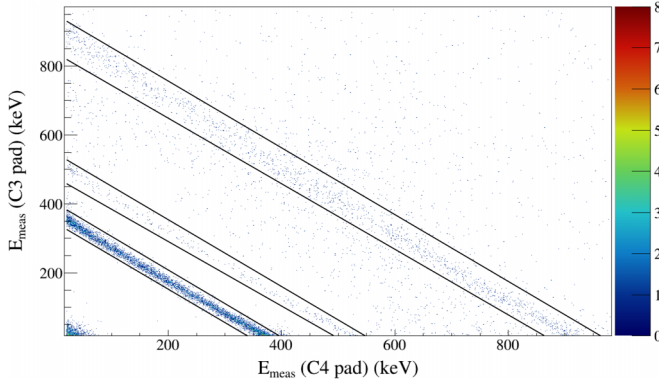| $E_p^{\text{c.m.}}$ (keV)	βp ratio (Absolute intensity) (%)		
	Thomas *et al.* [28]	Sun *et al.* [27]	This work
402.0(9)	4.75(32)	6.1(15)	9.57(17)
554(5)	0.69(25)	0.49(25)	0.43(3)
943.7(11)	1.63(20)	1.7(5)	2.35(9)

FIG. 7. Spectrum of ^{25}Si β-delayed proton energy loss detected in C3 vs. C4 pads, with a $M = 2$ condition applied in data analysis. Black lines are drawn to highlight the energies of interest.

of ^{25}Si which is presented in Fig. 5 is generated using a M = 1 condition, where the ionisation produced by an event takes place above only one pad, i.e., only one pad is hit. Even though, a disadvantage can arise considering the dimension of the central pads, C1–C5 (15×25 mm, each) which can be relatively small when compared with the mean free path in AB2 gas conditions of a proton with an energy E_p larger than several hundreds of keV. Some of the protons emitted over this pad have a chance of trespassing its boundaries and only a fraction of the signal will be recorded, with the remaining part being lost to the neighboring pad, i.e., the ionization is shared between two pads.

However, this type of event is not lost from the data analysis, but recovered with a M = 2 condition where only two neighboring pads are hit. An energy loss spectrum of such events between C3 and C4 pads can be seen in Fig. 7.

For higher energy particles with long tracks the signal will be shared between three or more neighboring pads; still, the signals are fully recovered. In this experiment, no events with a multiplicity M = 4 or higher were detected.

Recovering as much proton signals as possible by using M = 2, 3, etc.—where M = 3 could be constructed as C3-C4-CL4 or CL3-CL4-C4, etc. (see Fig. 3)—is very useful in calculating more precisely the βp branching ratios, while the M = 1 representation clears the positron background down to about 100 keV and allows a clear identification of low-energy resonances.

After energy calibration with known proton peaks from the decay of ^{25}Si we switched to the conditions described in Sec. II, selected ^{27}P and stopped it in the middle of AB2.

C. Proton energy correction

When assigning energy values for the proton groups, one should take care that the total energy measured by the detector, E_{meas}, is the sum of the energy of the proton, E_p, the energy of the recoil nucleus, E_{rec}, and the energy that the preceding beta particle deposited in the detector, E_β,

$$E_{\text{meas}} = E_p + \kappa E_{rec} + E_\beta$$
$$= \left(1 + \kappa \frac{M_p}{M_{rec}}\right) E_p + E_\beta, \quad (1)$$

where $M_{p,rec}$ are the masses of the proton and the recoil nucleus, respectively. A part of the energy of the recoil nucleus is lost in the excitation of the medium, and not on ionization of it and E_{rec} must be corrected with a factor κ, which was obtained from a TRIM [29] computation for the relevant recoil energies. More details on this procedure can be found in Ref. [17]. Most β^+ particles are minimally ionizing particles; the average amount of energy deposited in the gas above a pad by an emitted positron preceding the proton emission has been estimated using GEANT4 [30] simulations at ≈ 3 keV for this experiment.

IV. RESULTS

The β decay of ^{27}P is not well known. The ground state spin and parity of this nucleus is $J^\pi = 1/2^+$. It has a half-life of $T_{1/2} = 260(80)$ ms, a maximum available energy for β decay of $Q_{EC} = 11725(9)$ keV and $Q_{\epsilon p} = 4262(9)$ keV [6]. It β^+ decays to states in ^{27}Si. As mentioned before, the proton binding energy in ^{27}Si is $S_p(^{27}Si) = 7463.34(13)$ keV and its ground state spin and parity is $J^\pi = 5/2^+$. Four excited states in ^{27}Si above its proton binding energy are known from the β-delayed proton decay of ^{27}P, all assigned as $J^\pi = (1/2, 3/2)^+$. The βp branching ratio is quoted as <0.16% [13].

A. New low-energy proton groups

High energy protons previously observed [18,19] in the energy range 400 keV–900 keV, were also detected in this study, at 464(6), 615(6), and 736(6) keV (c.m. system). Even though in the study of McCleskey *et al.* [13] the detection of these three protons was also accomplished, the assigned energy values for them was done using the values from the study of Ognibene *et al.* [19].

By applying a M = 1 condition, the proton spectrum was cleared of positron background and allowed the discovery of five new proton groups located at 148(7), 182(7), 212(7), 261(6), and 388(6) keV, as it can be seen in Fig. 8 and listed in Table II. The measurement with ^{25}Si with the same setup shows that there is no instrumental background in this low energy region of the proton spectrum (Fig. 5). Even though the statistics are the lowest in the 200–230 keV energy region, following our data analysis we concluded that the peak identified at 212(7) keV is a real proton resonance, considering also that it can be paired with a previously known excited state in ^{27}Si. We see that the experimental setup provides significant improved results compared with any previous studies involving the decay of ^{27}P [13,18,19] in what concerns the peak energy resolution and positron background reduction. The spectrum of the energy loss from the positrons emitted at each ^{27}P decay is restricted to below 100 keV, making possible the identification of the very rare proton peaks for energies down to that value. Our proposed partial level scheme is presented in Fig. 9.

From the five new proton peaks we found in the spectra, only two of them can be be paired with a previously known excited state. The proton peak at $E_p = 148(7)$ keV, $E^* = 7840(7)$ keV can be paired with a previously known excited state at $E^* = 7837.9(2)$ keV [$J^\pi = (1/2)^+$] and
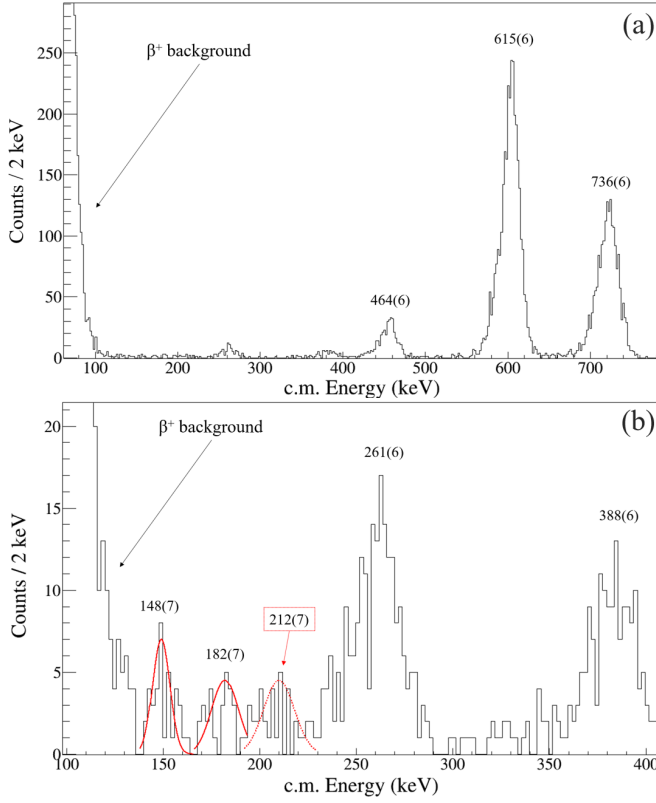
FIG. 8. β-delayed proton spectrum of ^{27}P. (a) Full range spectrum, obtained by applying a M = 1 condition on the most central pad, C3. Peak identification is done clearly and the positron background is reduced down to 90–100 keV. (b) Proton spectrum on the low-energy range, obtained by summing of C2–C4 pads (with M = 1 condition) and the M = 2 of C3 vs. C2 and C3 vs. C4, respectively.
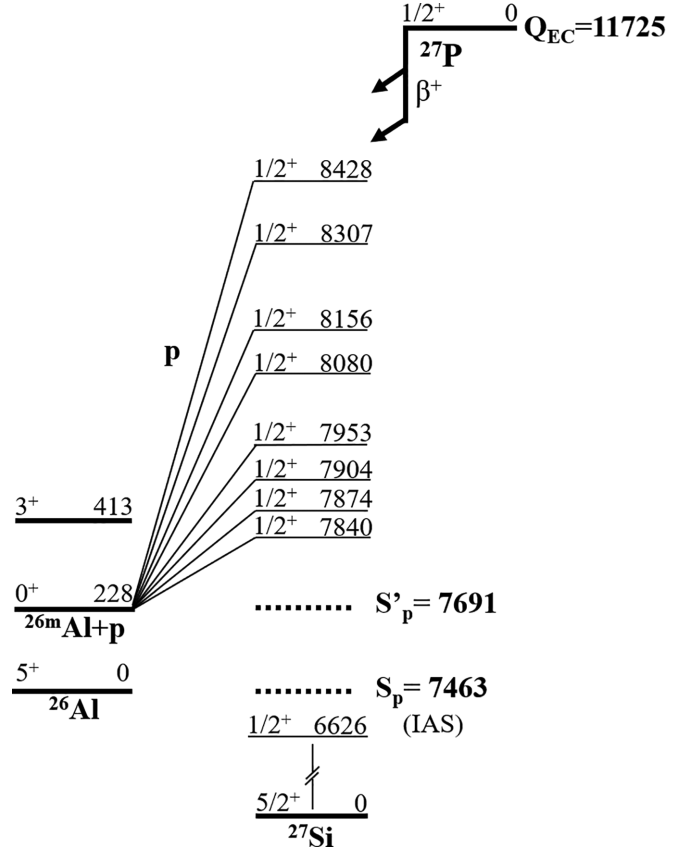

FIG. 9. Partial level scheme proposed for the β-delayed proton decay of ^{27}P. All the energy values are in keV.

$T_{1/2} < 0.7$ fs. The resonance at $E_p = 212(7)$ keV, $E^* = 7904(7)$ keV can be paired with a previously known level at $E^* = 7909.0(7)$ keV ($J^\pi = (3/2)^+$) [10]. This level's spin and parity were not definitively assigned, but we conclude to be $J^\pi = (1/2)^+$ as it will be explained in Sec. IV D.

Further, the relative intensities of the proton groups were calculated. We found the 615(6) keV group to be the most intense, contrary to the findings of Ognibene *et al.* [19]

study, where the most intense group was indicated to be the one of 736(6) keV. These results can also be found in Table II.

B. β-proton branching ratio determination

Another goal of this experiment was to calculate the β-proton branching ratio for each proton group,

$$B_i = \frac{N_i(p)/\varepsilon}{N(^{27}P)} \times \delta, \tag{2}$$

TABLE II. ^{27}P β-delayed proton groups and their properties. E_p reported in the c.m. system, E^* based on 7691.64(13) keV proton separation energy, βp branching ratio in absolute value.

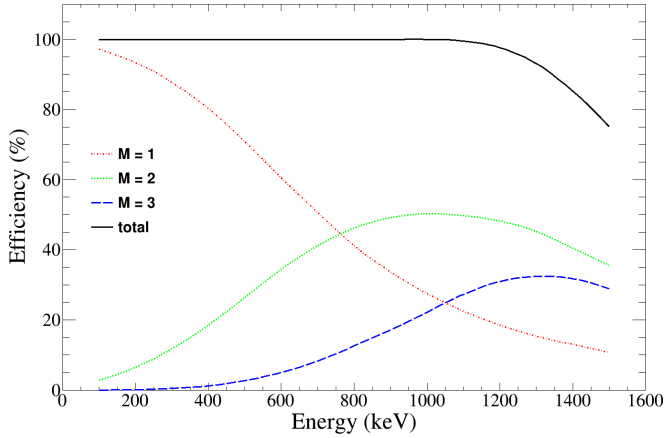| E_p(keV)		E^*(^{27}Si) (keV)		Rel. intensity (%)		βp ratio (abs. value)
present work	[19]	present work	[18,19]	present work	[19]	present work
148(7)	–	7840(7)	–	0.09	–	$5.8(8)\times10^{-7}$
182(7)	–	7874(7)	–	0.29	–	$1.8(2)\times10^{-6}$
212(7)	–	7904(7)	–	0.18	–	$1.12(12)\times10^{-6}$
261(6)	–	7953(6)	–	1.23	–	$8.3(3)\times10^{-6}$
388(6)	–	8080(6)	–	1.14	–	$1.00(4)\times10^{-5}$
464(6)	485(3)	8156(6)	8176(3)	7.94	9	$4.66(8)\times10^{-5}$
615(6)	637(2)	8307(6)	8328(2)	100	97	$5.88(3)\times10^{-4}$
736(6)	760(2)	8428(6)	8451(2)	96.79	100	$5.64(3)\times10^{-4}$

FIG. 10. Proton detection efficiency of AB2 detector, GEANT4 simulation, between 100–1500 keV. It can be seen that the sum of the first three multiplicities 100% up to ≈ 1100 keV.

FIG. 11. Decay time spectrum of ^{27}P. Only the beam-off period is represented in this picture.

where $N_i(p)$ is the number of protons of ith energy, ε is the detector efficiency for that proton energy and $N(^{27}P)$ is the total number of ^{27}P nuclei implanted over the pads. δ represents the summed contribution of corrections, such as data acquisition dead-time correction and decay losses during the implantation and pulsing switching periods; it was always very close to unity.

Proton detection efficiency of the experimental setup was estimated using a GEANT4 simulation and the results can be seen in Fig. 10. Detection efficiency is, of course, different for each multiplicity case. It reflects the fact that protons' paths can cover one or multiple pads, depending on the location of the decay event and the energy of the emitted proton. However, the summed efficiency of the first three multiplicity situations is $\varepsilon = 100\%$ up to nearly 1100 keV proton energy, as it can be seen from Fig. 10 and so the branching ratio does not depend anymore on the detection efficiency, but only on the number of protons detected and the number of ^{27}P nuclei implanted over the considered pads. As mentioned above, no M = 4 proton cases were found, so just identifying and counting all the events from M = 1, 2, 3 is sufficient to further calculate the values of the branching ratios. Also, the clean implantation that we obtained, allowed us to precisely determine the amount of ^{27}P which β-decayed. Note that all corrections due to the decays during collection and wait times in the cycles and of measurement dead-time where duly applied.

The lowest branching ratio measured was down to the value of $5.8(8)\times10^{-7}$, corresponding to the 148(7) keV proton group. A total proton branching ratio of $1.222(4)\times10^{-3}$ could be determined. The value we obtained is almost double than the previous determined one, of 0.7×10^{-3} [19], but in good agreement with the upper limit determined by the study of McCleskey *et al.* [13]. All the results are summarized in Table II.

C. Half-life of ^{27}P

Following the procedure explained above for the ^{25}Si data case, we managed to determine the half-life of ^{27}P. The value

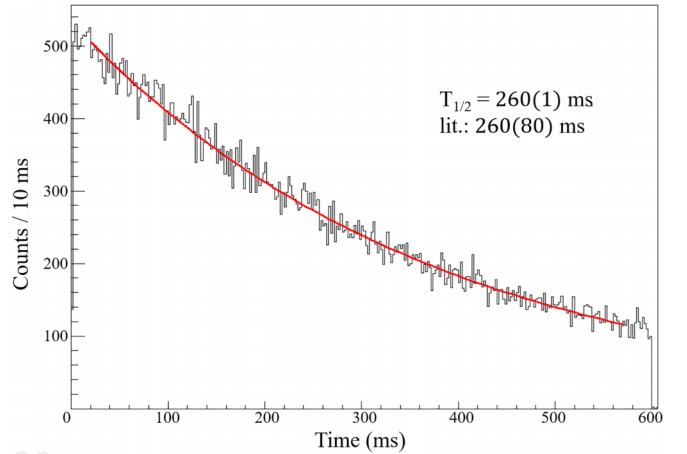$T_{1/2} = 260(1)$ ms obtained in this experiment is in agreement with the value of 260(80) ms obtained in the previous study of Aystö *et al.* [18] but has a considerably improved precision. The decay time spectrum can be seen in Fig. 11 and was obtained by gating on the decay energies of 464, 615, and 736 keV proton peaks; data from M = 1 and M = 2 were used.

D. ^{26m}Al(p, γ) ^{27}Si reaction rate

The resonant component of the reaction rate for isolated, narrow resonances is given by

$$N_A\langle\sigma v\rangle = 1.54\times10^{11}(\mu T_9)^{-3/2}$$
$$\times \sum_r (\omega\gamma)_r\exp(-11.605E_r/T_9), \quad (3)$$

in units of cm^{3}mol^{-1}s^{-1}. T_9 is the temperature in GK, E_r is the energy of the resonance in MeV, μ is the reduced mass in u, and $(\omega\gamma)_r$ is the resonance strength in MeV, given by

$$\omega\gamma = \frac{2J_r + 1}{(2J_{26Al} + 1)(2J_p + 1)}\frac{\Gamma_p\Gamma_\gamma}{\Gamma_{tot}}, \quad (4)$$

where Γ_p and Γ_γ are the partial widths of the proton and γ decays, Γ_{tot} is the total width (their sum), and $J_{r,p,^{26}Al}$ are the spins of the resonance, proton and ^{26}Al, respectively. Through the β decay of ^{27}P ($J^\pi = 1/2^+$), states in daughter nucleus ^{27}Si with $J^\pi = 1/2^+$ and $3/2^+$ are populated preferentially by allowed Gamow-Teller transitions. The states above the proton binding energy plus isomer excitation energy $S_{p'} = 7463.34 + 228.3 = 7691.64$ keV can further decay through the emission of a proton to the isomer $J^\pi = 0^+$ in ^{26}Al, and not to its $J^\pi = 5^+$ ground state, as the latter would require even angular momenta from $l = 4$ and up. Moreover, the proton decay from $3/2^+$ states in ^{27}Si to ^{26m}Al would imply transitions with relative angular momentum $l = 2$, highly inhibited by the extra centrifugal barrier (at low proton energies). That leads us to the conclusion that all resonances located by their p decay in our experiment (Table II) have spin and parity $J^\pi = 1/2^+$. In addition, in our experiment we had two HpGe detectors set to measure γ rays in coincidence with
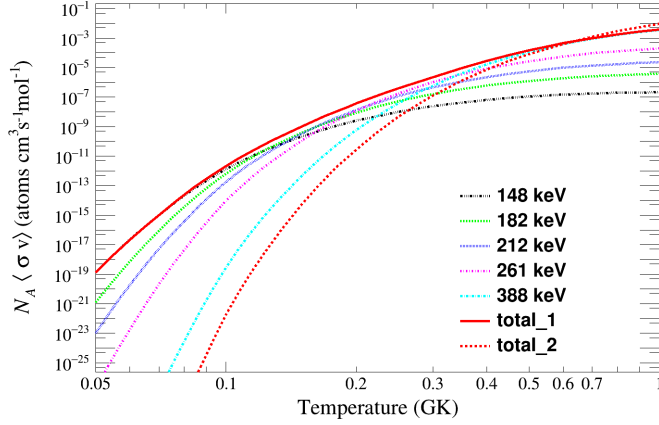
FIG. 12. Reaction rate contribution of the newly discovered resonances to the radiative proton capture on ^{26m}Al. The red solid line marked as "total_1" is the total contribution of these resonances, while the red dashed line represents the summed contribution of the high-energy resonances: 464, 615, and 736 keV.

TABLE III. Properties of resonances in ^{26}Al$(p, \gamma)^{27}$Si system.

E_{res} (keV)	Γ_p (eV)	Γ_γ (eV)	$\omega\gamma$ (eV)
148(7)	2.12×10^{-7}	$\leqslant 0.658$	2.12×10^{-7}
182(7)	5.40×10^{-6}	$\leqslant 0.658$	5.40×10^{-6}
212(7)	4.78×10^{-5}	$\leqslant 0.658$	4.78×10^{-5}
261(6)	7.23×10^{-4}	$\leqslant 0.658$	7.22×10^{-4}
388(6)	6.24×10^{-2}	$\leqslant 0.658$	5.70×10^{-2}
464(6)	0.35	$\leqslant 0.658$	0.23
615(6)	4.09	$\leqslant 0.658$	0.56
736(6)	16.39	$\leqslant 0.658$	0.63

low energy protons. There was no sign in the spectra of any γ ray emitted in coincidence with the proton peaks observed, therefore we exclude the populations of states above the 0^+ isomer in ^{26}Al.

For very low energy resonances $\Gamma_p \ll \Gamma_\gamma$, i.e., the γ decay dominates over the proton decay and the resonance strength depends almost entirely on the proton width, which can be expressed in its simplest form [31]

$$\Gamma_p = 2\frac{\hbar^2}{mR^2}PC^2S\theta_{pc}^2, \qquad (5)$$

where R is the nuclear radius, P is the barrier penetration factor, C^2 is the usual isospin Clebsch-Gordon coefficient, S is the spectroscopic factor and θ_{pc}^2 is the dimensionless single-particle reduced width. These latter factors depend on the actual structure of the decaying state and are difficult to calculate or even assess at these high excitation energies and level density. In our case, the spectroscopic factor S would measure the contribution of the single-particle $1s_{1/2}$ to the excited state in question in ^{27}Si. Therefore, we make below the somewhat usual assumption that $C^2S = 0.01$ in order to evaluate the proton decay widths before calculating the contribution of each resonance to the astrophysical reaction rate.

In Fig. 12 the contribution to the reaction rate of each of the five lowest resonances is plotted for the temperature range $T = 0.05$–1.0 GK. The solid red line shows the reaction rate where only the resonance energies up to 464 keV were included and the red dashed line shows the contribution of the higher energy resonances at 464, 615, and 736 keV. As we argued above that the excited states which correspond to proton decays in ^{27}Si have $J^\pi = 1/2^+$, the spin term in Eq. (4) is $\omega = 1$. Further, for the reaction rate evaluation, we adopted a value of 0.55 for θ_{pc}^2, as indicated in [31]. The Γ_p calculated values are listed in Table III. We assumed a typical lifetime of 1 fs for excited states of ^{27}Si in the $E^* = 7.7$–8.5 MeV region, which results in a maximum value of ≈ 0.658 eV for Γ_γ. This choice is guided by the lifetimes measured around this excitation energy [5], excited levels which were populated

mostly in the experiment performed by Lotay *et al.* [10]. This value was adopted for all resonances.

Figure 12 shows that for temperatures up to 0.4 GK, which are typical for classical novae explosions and static hydrogen burning, the low-energy resonances are the ones that contribute the most to the destruction of ^{26m}Al through radiative proton capture. There is a significant difference at low temperatures, of several orders of magnitude, between the summed contribution of the newly discovered proton resonances and the summed contribution of previously known proton resonances.

The destruction of ^{26m}Al takes place also through β decay. In Fig. 13, the curve indicates the conditions where the radiative capture reaction rate is of equal strength with the competing temperature- and proton-density-independent β^+ decay of ^{26m}Al. Above the curve the radiative proton capture is the dominant destruction mechanism, below it, β decay dominates. The corresponding density values are were determined using the following equation [32]:

$$\rho_\beta^{(p,\gamma)} = \frac{\ln 2}{T_{1/2}(^{26m}Al)N_A\langle\sigma v\rangle_{p,\gamma}} \, \text{g cm}^{-3}. \qquad (6)$$
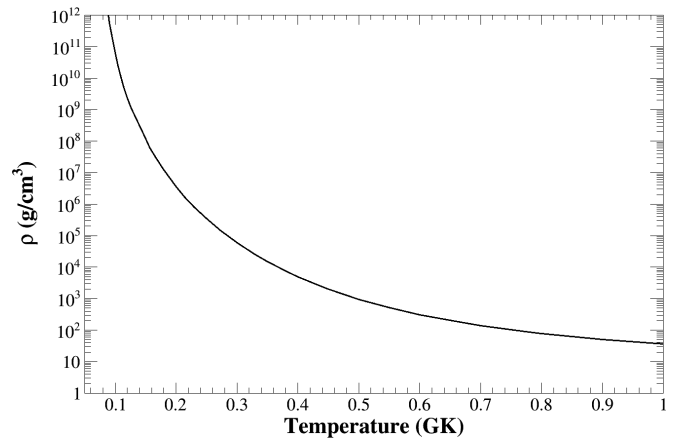

FIG. 13. Temperature and proton-density conditions at which the ^{26m}Al$(p, \gamma)^{27}$Si may play a role. The curve represents the equilibrium line between the rates for ^{26m}Al proton capture and ^{26m}Al β decay.

V. CONCLUSIONS

Using the β-delayed proton decay of ^{27}P and a specially designed gas detector with MicroMEGAS technology, we have been able to locate five new resonances that dominate the radiative proton capture reaction ^{26m}Al(p, γ) ^{27}Si at astrophysical important temperatures for the production and destruction of ^{26m}Al in cosmos. This method allowed to detect such low-energy protons, down to 150 keV, for the first time. Also, the technique we used proved to be, once again, suitable to study reactions involving β-delayed proton decay. It could also be used for β-delayed α-decay studies of exotic nuclei, like ^{16}N. The detection system involved, AstroBox2, demonstrated its capabilities, improved in the last years since its commissioning, to detect and measure protons of very low energy and provide a much reduced positron background than traditional silicon assemblies. It could measure protons with energies down to 100 keV and transitions with branching down into the 10^{-7} range.

The measurement of an error-improved half-life of $T_{1/2} = 260(1)$ ms for ^{27}P was also possible, along with a first time determination of βp branching ratios for each proton group separately. Using the five new resonances found, which we show to have $J^{\pi} = 1/2^+$ spin and parity, and assumptions about their widths, we re-evaluate the reaction rates in the temperature range $T_9 = 0.05$–1.0 GK, with a more pronounced interest in the classical novae explosions and hydrogen burning stage regions.

[1] R. Diehl *et al.*, The radioactive nuclei ^{26}Al and ^{60}Fe in the cosmos and in the solar system, Pub. Astron. Soc. Aust. **38**, e062 (2021).

[2] J. José and M. Hernanz, Nucleosynthesis in classical novae: CO versus one white dwarfs, Astrophys. J. **494**, 680 (1998).

[3] W. A. Mahoney *et al.*, Diffuse galactic gamma-ray line emission from nucleosynthetic Fe-60, Al-26, and Na-22-Preliminary limits from HEAO 3, Astrophys. J. **262**, 742 (1982).

[4] R. Diehl *et al.*, COMPTEL observations of galactic ^{26}Al emission, Astron. Astrophys. **298**, 445 (1995).

[5] M. Basunia and A. Hurst, Nuclear data sheets for A = 26, Nucl. Data Sheets **134**, 1 (2016).

[6] M. Wang, W. J. Huang, F. G. Kondev, G. Audi, and S. Naimi, The AME 2020 atomic mass evaluation (II). Tables, graphs and references, Chin. Phys. C **45**, 030003 (2021).

[7] A. E. Champagne *et al.*, The ^{26}Al(p,γ) ^{27}Si reaction at low stellar temperatures, Nucl. Phys. A **556**, 123 (1993).

[8] L. Buchmann *et al.*, The abundance of ^{26g}Al in the MgAl cycle, Nucl. Phys. A **415**, 93 (1984).

[9] C. Ruiz *et al.*, Measurement of the $E_{c.m.} = 184$ keV resonance strength in the ^{26g}Al(p,γ) ^{27}Si Reaction, Phys. Rev. Lett. **96**, 252501 (2006).

[10] G. Lotay, P. J. Woods, D. Seweryniak, M. P. Carpenter, R. V. F. Janssens, and S. Zhu, Identification of key astrophysical resonances relevant for the ^{26g}Al(p, γ) ^{27}Si reaction in Wolf-Rayet stars, AGB stars, and classical novae, Phys. Rev. Lett. **102**, 162502 (2009).

[11] S. D. Pain *et al.*, Constraint of the astrophysical ^{26g}Al(p, γ) ^{27}Si destruction rate at stellar temperatures, Phys. Rev. Lett. **114**, 212501 (2015).

[12] C. M. Deibel, J. A. Clark, R. Lewis, A. Parikh, P. D. Parker, and C. Wrede, Towards an experimentally determined ^{26m}Al(p,γ) ^{27}Si reaction rate in ONe novae, Phys. Rev. C **80**, 035806 (2009).

[13] E. McCleskey *et al.*, Simultaneous measurement of β-delayed proton and γ decay of ^{27}P, Phys. Rev. C **94**, 065806 (2016).

[14] S. Hallam *et al.*, Expoliting isospin symmetry to study the role of isomers in stellar environments, Phys. Rev. Lett. **126**, 042701 (2021).

[15] G. Lotay *et al.*, Radiative capture on nuclear isomers: Direct measurement of the ^{26m}Al(p,γ) ^{27}Si reaction, Phys. Rev. Lett. **128**, 042701 (2022).

[16] G. Lotay, P. J. Woods, D. Seweryniak, M. P. Carpenter, H. M. David, R. V. F. Janssens, and S. Zhu, Identification of analog states in the $T = 1/2$ $A = 27$ mirror system from low excitation energies to the region of hydrogen burning in the ^{26g,m}Al(p,γ) ^{27}Si reactions, Phys. Rev. C **84**, 035802 (2011).

[17] A. Saastamoinen *et al.*, Experimental study of β-delayed proton decay of ^{23}Al for nucleosynthesis in novae, Phys. Rev. C **83**, 045808 (2011).

[18] J. Aysto, X. J. Xu, D. M. Moltz, J. E. Reiff, J. Cerny, and B. H. Wildenthal, Beta-delayed proton decays of ^{27}P and ^{31}Cl: Gamow-Teller decays with large Q values, Phys. Rev. C **32**, 1700 (1985).

[19] T. J. Ognibene, J. Powell, D. M. Moltz, M. W. Rowe, and J. Cerny, Additional results from the β-delayed proton decays of ^{27}P and ^{31}Cl, Phys. Rev. C **54**, 1098 (1996).

[20] R. E. Tribble, R. H. Burch, and C. A. Gagliardi, Mars: A momentum achromat recoil spectrometer, Nucl. Instrum. Methods Phys. Res. A **285**, 441 (1989).

[21] Y. Giomataris *et al.*, MICROMEGAS: A hig-granularity position-sensitive gaseous detector for high particle-flux environments, Nucl. Instrum. Methods Phys. Res. A **376**, 29 (1996).

[22] J. P. Wallace *et al.*, β-delayed proton-decay study of ^{20}Mg and its implications for the ^{19}Ne(p,γ) ^{20}Na breakout reaction in X-ray bursts, Phys. Lett. B **712**, 59 (2012).

[23] A. Saastamoinen, A. Kankainen, and L. Trache, Beta-decay of ^{31}Cl: An indirect probe of the ^{30}P(p,γ) ^{31}S reaction. Present status and future perspectives, Eur. Phys. J. Plus **131**, 272 (2016).

[24] R. Chzyh, Measurement of β-delayed protons from ^{35}K relevant to the ^{34}Cl$^{g,m}(p,\gamma)$ ^{35}Ar, Ph.D. thesis, Texas A&M University (2019).

[25] A. Saastamoinen *et al.*, AstroBox2 - Detector for low-energy β-delayed particle detection, Nucl. Instrum. Methods Phys. Res. B **376**, 357 (2016).

[26] E. Pollacco *et al.*, AstroBox: A novel detection system for very low-energy protons from β-delayed proton decay, Nucl. Instrum. Methods Phys. Res. A **723**, 102 (2013).

[27] L. J. Sun *et al.*, ^{25}Si β^+-decay spectroscopy, Phys. Rev. C **103**, 014322 (2021).

[28] J. C. Thomas *et al.*, Beta-decay properties of ^{25}Si and ^{26}P, Eur. Phys. J. A **21**, 419 (2004).

[29] J. F. Ziegler *et al.*, SRIM-The stopping and range of ions in matter (2010), Nucl. Instrum. Methods Phys. Res. B **268**, 1818 (2010).

[30] J. Allison *et al.*, Recent developments in Geant4, Nucl. Instrum. Methods Phys. Res. A **835**, 186 (2016).

[31] C. Iliadis, Proton single-particle reduced widths for unbound states, Nucl. Phys. A **618**, 166 (1997).

[32] A. Banu, T. Al-Abdullah, C. Fu, C. A. Gagliardi, M. McCleskey, A. M. Mukhamedzhanov, G. Tabacaru, L. Trache, R. E. Tribble, Y. Zhai, F. Carstoiu, V. Burjan, and V. Kroha, Astrophysical *s* factor for the radiative capture ^{12}N$(p,\gamma)^{13}$O determined from the ^{14}N$(^{12}$N,^{13}O$)^{13}$C proton transfer reaction, Phys. Rev. C **79**, 025805 (2009).